

# Evidence for *S*-nitrosothiol-dependent changes in fibrinogen that do not involve transnitrosation or thiolation

Shirin Akhter<sup>\*†</sup>, Arianna Vignini<sup>\*</sup>, Zhong Wen<sup>‡</sup>, Ann English<sup>§</sup>, Peng G. Wang<sup>‡</sup>, and Bulent Mutus<sup>\*†</sup>

<sup>\*</sup>Department of Chemistry and Biochemistry, University of Windsor, Windsor, ON, Canada N9B 3P4; <sup>‡</sup>Department of Chemistry, Wayne State University, Detroit, MI 48202; and <sup>§</sup>Department of Chemistry and Biochemistry, Concordia University, Montreal, QC, Canada H3G 1M8

Edited by Louis J. Ignarro, University of California School of Medicine, Los Angeles, CA, and approved May 17, 2002 (received for review March 7, 2002)

*S*-nitrosoglutathione (GSNO, 50  $\mu$ M) inhibited the initial rate of thrombin-catalyzed human and bovine fibrinogen polymerization by  $\approx$ 50% to 68% respectively. Inhibition was also observed with other structurally varied *S*-nitrosothiols (RSNOs) including sugar derivatives of *S*-nitroso-*N*-acetylpenicillamine (SNAP). The fact that the same concentration of GSNO had no effect on thrombin-dependent hydrolysis of tosylglycylprolylarginine-4-nitroanilide acetate suggested that this inhibition was due to GSNO-induced changes in fibrinogen structure. This result was confirmed by CD spectroscopy where GSNO or *S*-nitrosohomocysteine increased the  $\alpha$ -helical content of fibrinogen by  $\approx$ 15% and 11%, respectively. *S*-carboxymethylamido derivatives of glutathione or homocysteine had no effect on the fibrinogen secondary structure. The GSNO-dependent secondary structural effects were reversed on gel filtration chromatography, suggesting that the effects were allosteric. Further evidence for fibrinogen–GSNO interactions was obtained from GSNO-dependent quenching of the intrinsic fibrinogen Trp fluorescence and the perturbation of the GSNO circular dichroic absorbance as a function of [fibrinogen]. The  $K_{d}$ s of 3 to 10  $\mu$ M for fibrinogen–GSNO interactions with a stoichiometry of 2:1 (GSNO:fibrinogen) were estimated from isothermal titration calorimetry and fluorescence quenching, respectively. These results suggest that RSNOs induce changes to fibrinogen structure by interacting at specific aromatic rich domains. Three such putative RSNO-binding domains have been identified in the unordered, aromatic residue-rich C-termini of the  $\alpha$ -chains of fibrinogen.

Fibrinogen is a multidomain glycoprotein (340 kDa) involved in blood coagulation. Its main function is the formation of the three-dimensional network of fibrin fibers giving rise to the blood clot. It consists of two identical subunits, each of which is formed by three nonidentical polypeptide chains,  $\alpha$ ,  $\beta$ , and  $\gamma$  ( $\alpha\beta\gamma$ )<sub>2</sub>. Fibrinogen contains a total of 29 disulfide bonds and no free sulfhydryl groups. Recently, crystal structures of native chicken fibrinogen (1), as well as a modified bovine protein (2), have been reported. The clot formation is initiated by thrombin, a serine protease that catalyzes the transformation of fibrinogen into fibrin by removing small polar peptides, fibrinopeptides A and B, from the parent molecule.

*S*-nitrosothiols (RSNO) are formed by the reaction of small molecular weight and protein thiols either with the nitrosonium ion (NO<sup>+</sup>) or by NO under aerobic conditions (3). Apart from being cellular sources of NO, they also prolong its half-life (4). RSNOs are involved in signaling pathways, in immune responses, and in the actions of nitrovasodilating compounds (5, 6). RSNOs have been shown to modulate the activity of numerous enzymes (7–10) by participating in transnitrosation or *S*-thiolation reactions.

In this study, we report that the significant structural and functional RSNO-dependent changes in fibrinogen apparently do not involve NO or thiol exchange. These RSNO-dependent alterations in protein structure are postulated to result from *S*–NO interactions with aromatic protein side chains. Evidence presented in support of this postulate include the perturbation of

RSNO CD spectra by fibrinogen and RSNO-dependent fluorescence quenching of Trp fluorescence, as well as thermodynamic data from isothermal titration calorimetry (ITC).

## Materials and Methods

**Materials.** Crystallography grade human thrombin and fibrinogen were purchased from Haematologic Technologies (Essex Junction, VT), bovine fibrinogen, fraction I, type I-S, bovine thrombin, 5,5'-dithiobis-2-nitrobenzoate (DTNB), glutathione (GSH),  $\alpha$ -tocopherol, and iodoacetamide were purchased from Sigma-Aldrich. Chromozym TH (tosylglycylprolylarginine-4-nitranilide acetate) was purchased from Roche Molecular Biochemicals. PTIO (2-phenyl-4,4,5,5-tetramethylimidazoline-1-oxyl-3-oxide) was purchased from OxisResearch (Portland, OR).

**Synthesis of GSNO.** GSH (Sigma) was dissolved in ice-cold 0.5 M HCl. Equimolar sodium nitrite was added, and the reaction was carried out in the dark at 4°C for 40 min. The pH of the reaction mixture was adjusted to 7.4. The product was precipitated from the solution by the slow addition of cold acetone and washed successively with ice-cold acetone, water, and diethyl ether. *S*-nitrosohomocysteine (HCysNO) was synthesized by the same procedure.

**Synthesis of RSNOs and Pyrrolidinium Diazenium Diolate (Pyrrolidinium NONOate).** Captopril-SNO, glucose-1-*S*-nitroso-*N*-acetylpenicillamine (glucose-1-SNAP), fructose-1-SNAP, *S*-nitroso-BSA (BSA-NO), and pyrrolidinium NONOate were synthesized according to previously published methods (11–15).

**Preparation of Pyrrolidinium NONOate Solution.** Pyrrolidinium NONOate was dissolved in methanol in a drum vial and sealed with a septum. Pyrrolidinium NONOate solution was degassed with nitrogen to prevent the reaction of released NO with oxygen. The pyrrolidinium NONOate solutions were made fresh before use.

**Fibrinogen Polymerization.** Kinetic measurements of fibrinogen polymerization were carried out by using an Agilent (Palo Alto, CA) 8453 UV-visible spectrophotometer with a Pelletier temperature controller (25°C). Fibrinogen was first dissolved in 50  $\mu$ l of glycine-NaOH buffer (50 mM, pH 8.5). Once solubilized, the fibrinogen was diluted in PBS (NaCl 0.137 M/KCl 2.7 mM/Na<sub>2</sub>HPO<sub>4</sub> 10 mM/KH<sub>2</sub>PO<sub>4</sub> 1.76 mM, pH 7.4) to a final concentration of 0.38  $\mu$ M. The polymerization was initiated by

This paper was submitted directly (Track II) to the PNAS office.

Abbreviations: RSNO, *S*-nitrosothiol; ITC, isothermal titration calorimetry; PTIO, 2-phenyl-4,4,5,5-tetramethylimidazoline-1-oxyl-3-oxide; SNAP, *S*-nitroso-*N*-acetylpenicillamine; GSNO, *S*-nitrosoglutathione; HCysNO, *S*-nitrosohomocysteine; DTNB, 5,5'-dithiobis-2-nitrobenzoate; GSH, glutathione; GSSG, glutathione disulfide.

<sup>†</sup>To whom reprint requests should be addressed at: Department of Chemistry and Biochemistry, University of Windsor, 401 Sunset Avenue, Windsor, ON, Canada N9B 3P4. E-mail: mutusb@uwindsor.ca or akhter@server.uwindsor.ca.

the addition of 0.03  $\mu\text{M}$  thrombin. The turbidity of the solution was measured at 660 nm. The initial rates were calculated from the  $\Delta\text{OD}$  within the first 20 s subsequent to mixing of the reagents. When the polymerization was performed in the presence of *S*-nitrosoglutathione (GSNO), the fibrinogen sample was incubated with GSNO for 10 min in the dark.

**Thrombin Assay.** The activity of thrombin was determined with the colorimetric pseudo-substrate Chromzym TH. Thrombin (0.6  $\mu\text{M}$ ), either preincubated with 50  $\mu\text{M}$  GSNO for 15 min or not, was added to a 0.2 mM solution of Chromzym TH in PBS (25°C). The absorbance (405 nm) was measured as a function of time in the spectrometer described above. The blank hydrolysis rate was subtracted from the enzymatic rate.

**CD Measurements.** Fibrinogen (0.3  $\mu\text{M}$ ) in PBS buffer was placed in a 1-cm quartz cuvette, the CD spectra were measured over the wavelength region of 190 nm to 260 nm (protein secondary structure) or 500 nm to 600 nm (RS-NO environment) in an Aviv (Aviv Associates, Lakewood, NJ) CD spectrometer model 62A DS. Each spectrum is an average of three different scans obtained by collecting data at 1-nm intervals with an integration time of 10 s at a constant temperature of 25°C. The secondary structure composition was determined with the aid of CD neural network to deconvolution software (16).

**Free Thiol Content.** The free thiol content of the samples was determined colorimetrically with the aid of DTNB ( $\epsilon_{412} = 13,600 \text{ M}^{-1}\cdot\text{cm}^{-1}$ ).

**Blockage of Free Thiols with Iodoacetamide.** GSH or HCys (5 mmol) was dissolved in Tris-acetate buffer (50 mM, pH 8.5). To this solution, 5 mmol iodoacetamide was added. The mixture was stirred at room temperature for 2 h. The solutions were then diluted appropriately in PBS and used without further purification.

**Fluorescence Measurements.** The intrinsic Trp fluorescence spectra of fibrinogen solutions in PBS were measured with the aid of a Perkin-Elmer fluorometer. The samples were excited at 290 nm. The emission spectrum 300 nm to 400 nm was monitored as a function of [GSNO]. The absorbance of the solutions at 290 nm did not exceed 0.1. Fractional quenching at a given [GSNO] was estimated by dividing this value by the maximal quenching obtained at the largest [GSNO]. These data were then fitted to a saturation function ( $\Delta F/\Delta F_{\text{tot}} = [\text{GSNO}]/(K_d + [\text{GSNO}])$ ) to estimate the  $K_d$ .

**Isothermal Titration Calorimetry.** ITC measurements were performed at 25°C by using MicroCal VP ultrasensitive titration calorimeter. Fibrinogen solution was dialyzed extensively against PBS. Then the dialyzed sample (2.6  $\mu\text{M}$ ) was added to the 1.4-ml calorimeter sample cell. GSNO solution (0.6 mM in PBS buffer) was injected to the sample cell in 1- to 5- $\mu\text{l}$  aliquots at 4- to 8-min intervals. The heat of reaction per injection ( $\mu\text{cal/s}$ ) was determined by integration of peak areas using ORIGIN software (Microcal Software, Northampton, MA). The heat of dilution was determined from the baseline at the end of titration and subtracted from the observed heat of binding. Heat evolved per mole of substrate injected was plotted against the GSNO/fibrinogen molar ratio.  $\Delta H^\circ$ , the stoichiometry of binding ( $n$ ), and the dissociation constant ( $K_d$ ) were estimated from the best fit. The Gibbs free energy of binding [ $\Delta G^\circ = RT \ln(1/K_d)$ ] and the entropy of binding ( $T\Delta S^\circ = \Delta H^\circ - \Delta G^\circ$ ) were calculated from the experimental values.

## Results

**GSNO Inhibits Thrombin-Catalyzed Fibrinogen Polymerization.** Thrombin catalyzes the transformation of fibrinogen into fibrin by removing the small polar peptides, fibrinopeptides A and B,

from the parent molecule. Removal of the peptides uncovers the knobs that lead to the polymerization of fibrinogen. This process can be monitored *in vitro* by measuring the increase in turbidity (660 nm) of a fibrinogen solution in the presence of catalytic amounts of thrombin. As can be seen in Fig. 1A (squares) the initial rate of bovine fibrinogen polymerization ( $2.5 \times 10^{-5}/\text{s}$ ) decreased by  $\approx 60 \pm 8\%$  (circles) and  $\approx 68 \pm 10\%$  (triangles) in the presence of 20  $\mu\text{M}$  and 50  $\mu\text{M}$  GSNO, respectively. These experiments were repeated with human fibrinogen and thrombin where 20  $\mu\text{M}$  and 50  $\mu\text{M}$  GSNO resulted in  $\approx 43 \pm 7\%$  and  $\approx 50 \pm 8\%$  inhibition, respectively (Fig. 1B).

**Glutathione Disulfide (GSSG) and Pyrrolidinium NONOate Have No Effect on Fibrinogen Polymerization.** There is a possibility that the observed inhibition of initial rate of fibrinogen polymerization is due to  $\text{NO}_x$ -protein reactions from thermally or photolytically released NO from the RSNOs used. Another possibility is that GSSG, which could be formed as a result of the loss of NO from GSNO, could be affecting the polymerization. To test for these possibilities, fibrinogen polymerizations were carried out in the presence of pyrrolidinium NONOate, which is known to rapidly release NO in solution ( $t_{1/2} = 1.8 \text{ s}$ ) or GSSG. However these compounds had no effect on the initial rates of fibrinogen polymerization (Fig. 1C).

**NO Scavenger PTIO Has No Effect on GSNO Inhibition of Fibrinogen Polymerization.** To further eliminate the possibility that the observed inhibition is due to NO released from the RSNOs or other  $\text{NO}_x$  species subsequently formed, the polymerizations were repeated in the presence of 50  $\mu\text{M}$  PTIO as a NO scavenger (17). In addition, these solutions contained  $\approx 5 \mu\text{M}$   $\alpha$ -tocopherol to scavenge any  $\text{NO}_2$  that might be produced. In the presence of PTIO/ $\alpha$ -tocopherol GSNO (50  $\mu\text{M}$ ) inhibited polymerization by  $\approx 60 \pm 9\%$  (Fig. 1D). This result is yet another line of evidence that NO or  $\text{NO}_x$  species are not causing the inhibition.

**GSNO Has No Effect on Thrombin.** To examine whether GSNO affected thrombin or fibrinogen, thrombin was incubated with 50  $\mu\text{M}$  GSNO for 15 min in the dark. The thrombin activity was then measured with the protease pseudosubstrate Chromozym TH. It was found that the activity of thrombin was not affected by GSNO because the initial rates of Chromozym TH hydrolysis were indistinguishable with ( $7.31 \times 10^{-3} \pm 5.57 \times 10^{-5}$ )/s or without GSNO ( $7.33 \times 10^{-3} \pm 1.8 \times 10^{-4}$ )/s. It is also conceivable that the RSNOs did not inhibit thrombin but did inhibit contaminating amounts of factor XIII, which has an active site thiol that can be inactivated via transnitrosation (18). This result does not appear to be the case because the fibrinogen (human and bovine) polymerization rates in the absence of thrombin were negligible ( $7 \times 10^{-6} \pm 8 \times 10^{-6} \text{ s}^{-1}$ ).

Other structurally diverse RSNOs also inhibited the process (Table 1) with similar  $\text{IC}_{50\text{s}}$  within experimental error, and the maximal inhibition varied from 68% in the case of GSNO to  $\approx 43\%$  with fructose-1-SNAP.

**GSNO and HCysNO Affect Fibrinogen Secondary Structure.** Fibrinogen (bovine and human) secondary structure was monitored by CD as a function of [GSNO] (Fig. 2A and B). GSNO increased the negative ellipticity at 207 nm and decreased the positive ellipticity at  $\approx 190 \text{ nm}$ . This change appears to be RSNO specific because *S*-amidomethyl-GSH (Fig. 2C) or *S*-amidomethyl-HCys (data not shown) failed to alter the CD spectrum of fibrinogen.

The GSNO-dependent effect on fibrinogen secondary structure was reversible because the fibrinogen CD spectrum was very close to that of native spectrum subsequent to separation of GSNO from fibrinogen by FPLC (Fig. 2D).

On deconvolution, the GSNO-dependent change in the CD spectrum corresponded to a  $\approx 15\%$  increase in helicity at the

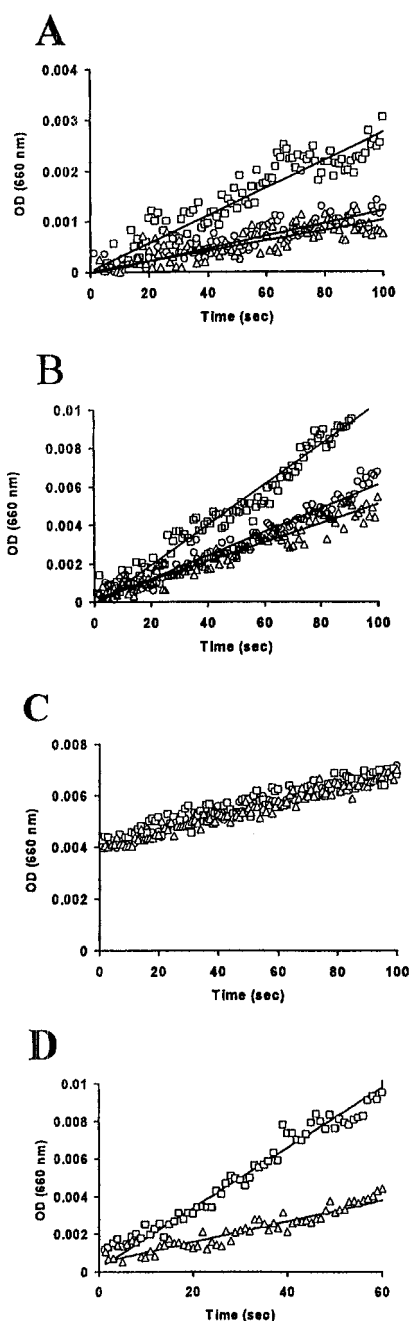


**Fig. 1.** The effect of GSNO on thrombin catalyzed fibrinogen polymerization. (A) The turbidity of the solution of bovine fibrinogen (0.38  $\mu\text{M}$ ) plus thrombin (0.03  $\mu\text{M}$ ) was monitored as a function of time at 660 nm in the presence of (□) buffer alone, (○) 20  $\mu\text{M}$  GSNO, and (△) 50  $\mu\text{M}$  GSNO. (B) The turbidity of the solution of human fibrinogen (0.38  $\mu\text{M}$ ) plus thrombin (0.003  $\mu\text{M}$ ) was monitored as a function of time at 660 nm in the presence of (□) buffer alone, (○) 20  $\mu\text{M}$  GSNO, and (△) 50  $\mu\text{M}$  GSNO. (C) The turbidity of the solution of fibrinogen (0.38  $\mu\text{M}$ ) plus thrombin (0.03  $\mu\text{M}$ ) was monitored as a function of time at 660 nm in the presence of (□) buffer alone, (○) 10  $\mu\text{M}$  pyrrolidinium-NONOate, and (△) 50  $\mu\text{M}$  GSSG. (D) The turbidity of the solution of human fibrinogen (0.38  $\mu\text{M}$ ) plus thrombin (0.003  $\mu\text{M}$ ) was monitored as a function of time at 660 nm in the presence of buffer containing the following: (□) 5  $\mu\text{M}$   $\alpha$ -tocopherol 50  $\mu\text{M}$  PTIO, and (△) 50  $\mu\text{M}$  GSNO, 5  $\mu\text{M}$   $\alpha$ -tocopherol, and 50  $\mu\text{M}$  PTIO.

expense of  $\approx 10\%$  loss in  $\beta$  sheet and  $\approx 5\%$  decrease in random coil content. Similar secondary structural effects were observed with another RSNO, HCysNO (data not shown).

**Table 1. Apparent inhibition constants between RSNOs and fibrinogen**

RSNO	Apparent $\text{IC}_{50}$ , $\mu\text{M}$	Maximal inhibition, % of control
GSNO	$4.0 \pm 1.0$	68
SNAP	$5.0 \pm 2.1$	64
Captopril-SNO	$6.5 \pm 2.2$	46
Glucose-1-SNAP	$7.5 \pm 2.7$	56
Fructose-1-SNAP	$6.0 \pm 2.3$	43
BSA-NO	$7.0 \pm 3.4$	46

An initial rate of fibrinogen polymerization catalyzed by thrombin in the presence of RSNO was determined by following the same experimental conditions described in Fig. 1 (see *Materials and Methods*). Fractional inhibition at a certain [RSNO] was estimated by dividing each single inhibition by the maximum inhibition obtained at the largest [RSNO]. Then the values were fitted to a saturation function to obtain the apparent inhibition constants ( $\text{IC}_{50}$ ). Fibrinogen polymerization rates were monitored at RSNO concentration range of 0.1–100  $\mu\text{M}$ . Values are the means  $\pm$  SD from five experiments.

**There Is No Detectable NO Produced During the CD Experiment.** The S–NO bond is photolabile. It is therefore conceivable that the observed conformational changes result from NO generated from photolysis of S–NO, by the monitoring beam during the CD experiment, which might react with protein functional groups. This possibility was tested by inserting a NO-specific electrode (ISO-NO, Mark II; WPI Instruments, Waltham, MA) into the cuvette containing a solution of GSNO (0.05  $\mu\text{mol}$ ) plus fibrinogen, in the sampling chamber of the CD spectrometer. There was no detectable NO produced during the CD experiment (data not shown).

**GSNO Quenches the Intrinsic Trp Fluorescence of Fibrinogen in a Saturable Manner.** The intrinsic Trp fluorescence spectrum was monitored as a function of [GSNO]. The fibrinogen fluorescence was quenched in a saturable manner (Fig. 3A), indicating that the process is not due to collisional quenching. The fit of the quenching data to a saturation function resulted in estimated  $K_d$  of 10  $\mu\text{M}$ . In an effort to estimate the stoichiometry of GSNO/fibrinogen interaction, 100  $\mu\text{M}$  fibrinogen was titrated with [GSNO]. Because this is above the estimated  $K_d$ , the fluorescence quenching should represent stoichiometric binding. Under these conditions, the quenching profile was characterized by two slopes that when extrapolated gave an approximate ratio of 2:1 (GSNO/fibrinogen) (Fig. 3B).

**Fibrinogen Perturbs the S–NO CD Spectrum.** The CD absorption spectrum (550 nm) of RSNOs is spectrally well separated from that resulting from protein secondary structure (19). Low molecular weight RSNOs where the —SNO is free to rotate, have a strong CD absorption in the 500- to 600-nm region. However, this signal is lost if rotation is restricted as is the case in serum albumin-NO (19). When 25  $\mu\text{M}$  fibrinogen (50  $\mu\text{M}$  in estimated GSNO site concentration) was added to 100  $\mu\text{M}$  GSNO, the magnitude of GSNO-CD spectrum decreased by  $\approx 1/2$  (Fig. 3C). This result is an indication that the rotational freedom of the SNO moiety is restricted on interacting with fibrinogen. In addition, the CD studies confirm the 2 to 1 GSNO/fibrinogen stoichiometry determined by the fluorescence titrations (Fig. 3B).

**ITC.** In an effort to characterize the GSNO-fibrinogen interactions by another independent technique, 2.6  $\mu\text{M}$  fibrinogen was titrated in a calorimeter with 1- $\mu\text{l}$  to 5- $\mu\text{l}$  aliquots of GSNO (0.6 mM in syringe concentration). The data were best fitted with two binding sites/fibrinogen with a  $K_d$  of  $3.31 \pm 0.9$   $\mu\text{M}$  (Fig. 4). The

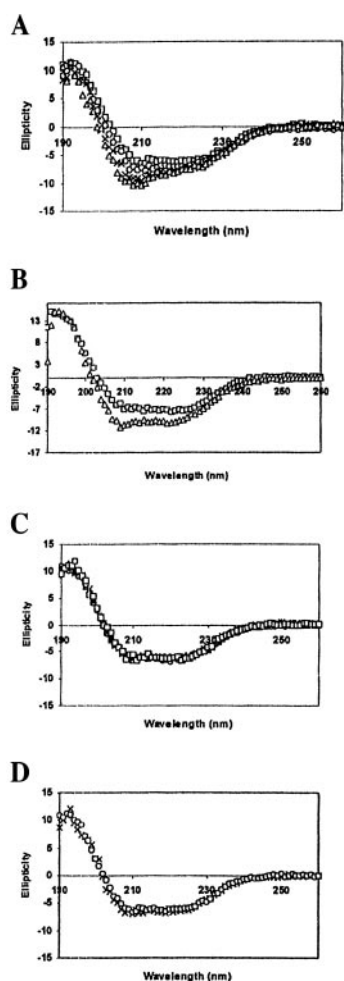


**Fig. 2.** The effect of GSNO and HCysNO on fibrinogen secondary structure. (A) The far UV CD spectra of bovine fibrinogen ( $0.3 \mu\text{M}$ ) were measured in the presence of ( $\square$ ) buffer alone, ( $\circ$ )  $25 \mu\text{M}$  GSNO, ( $\times$ )  $30 \mu\text{M}$  GSNO, and ( $\Delta$ )  $50 \mu\text{M}$  GSNO. (B) The far UV CD spectra of human fibrinogen ( $0.03 \mu\text{M}$ ) were measured in the presence of ( $\square$ ) buffer alone and ( $\Delta$ )  $50 \mu\text{M}$  GSNO. (C) The far UV CD spectra of fibrinogen ( $0.3 \mu\text{M}$ ) were measured in the presence of ( $\Delta$ ) buffer alone, ( $\circ$ )  $25 \mu\text{M}$  *S*-amidomethyl-GSH, ( $\square$ )  $30 \mu\text{M}$  *S*-amidomethyl-GSH, and ( $\times$ )  $50 \mu\text{M}$  *S*-amidomethyl-GSH. (D) The far UV CD spectra of fibrinogen ( $0.3 \mu\text{M}$ ) were measured in the presence of ( $\times$ ) buffer alone and after exposure to GSNO for 10 min followed by chromatography on Sephadex G-25 ( $\circ$ ). The depicted CD spectra (A–D) are representative of the average of four different experiments. In each experiment, the average of three different scans was recorded. SD values are within the dimension of the symbols used in the figures.

process appears to be entropy driven, with a  $\Delta S$  of 63.7 and a  $\Delta H$  of 1.12 kcal/mol.

### Discussion

There have been several reports on RSNO-dependent inhibition of blood clot formation (18) and platelet aggregation (20–23). In all of these cases, the mechanism of inhibition has been attributed to either the NO-mimicking activity of RSNOs in triggering the NO/cGMP pathway or has involved the transnitrosation or *S*-thiolation of an essential free thiol(s) on the proteins participating in thrombosis or platelet activation. The activity of several enzymes not involved in hemostasis—namely creatine kinase (7), papain (8), protein tyrosine phosphatases (9), and human rhinovirus 3C protease (10)—have also been shown to be attenuated by RSNO-dependent transnitrosation or *S*-thiolation.

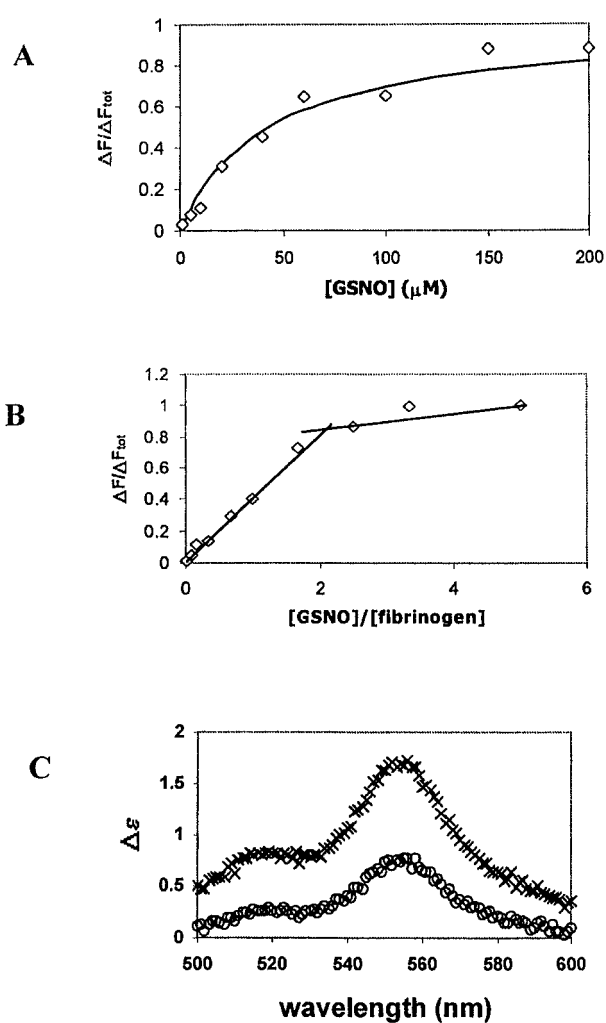


**Fig. 3.** (A) The effect of GSNO on fluorescence emission of fibrinogen. The intrinsic Trp fluorescence spectra of fibrinogen solutions. The emission spectrum 300 nm to 400 nm was monitored as a function of [GSNO]. Fractional quenching at a given [GSNO] was estimated by dividing this value by the maximal quenching obtained at the largest [GSNO]. These data were then fitted to a saturation function ( $\Delta F/\Delta F_{\text{tot}} = [\text{GSNO}]/(K_d + [\text{GSNO}])$ ) to estimate the apparent  $K_d$ . The absorbance of the solutions at 290 nm did not exceed 0.1. (B) Determination of fibrinogen:GSNO stoichiometry from fibrinogen fluorescence quenching as a function of [GSNO]. The fluorescence emission at 330 nm ( $\lambda$  excitation 290 nm) of a  $100\text{-}\mu\text{M}$  solution of fibrinogen was monitored as a function of [GSNO] in a  $0.2\text{-cm}$  path length fluorescence cuvette. Fractional quenching at a given [GSNO] was estimated by dividing this value by the maximal quenching obtained at the largest [GSNO]. (C) The effect of fibrinogen on [GSNO] CD spectrum. The CD spectra  $100 \mu\text{M}$  GSNO ( $\times$ ) plus  $25 \mu\text{M}$  fibrinogen ( $\circ$ ).

In the present study, GSNO was observed to inhibit thrombin-catalyzed fibrinogen polymerization. Thrombin did not appear to be affected because the initial rates of Chromozym TH hydrolysis were unchanged after a 15-min exposure to GSNO. This result suggested that the GSNO inhibited polymerization via its actions on fibrinogen. This finding was intriguing because all of the thiols in fibrinogen are involved in disulfide bridges. Before proceeding further, we ensured that the GSNO samples did not contain any free thiols (i.e., unreacted GSH). The amount of free thiol was determined by DTNB titrations to be  $<1\%$  of the [GSNO], and these were blocked by iodoacetamide. Without the S-NO moiety, *S*-amidomethyl-GSH or *S*-amidomethyl-HCys did not perturb fibrinogen secondary structure as

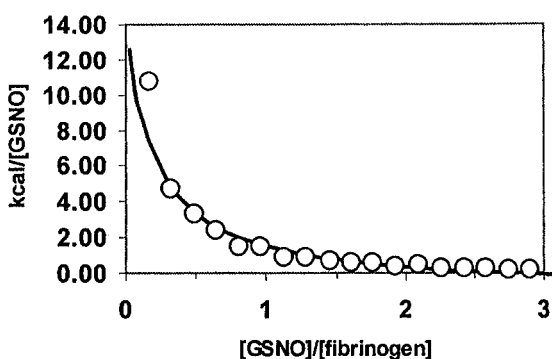


**Fig. 4.** Determination of dissociation constant ( $K_d$ ) between fibrinogen and GSNO by using isothermal titration calorimetry. A fibrinogen sample (2.6  $\mu$ M) was taken into the 1.4-ml calorimeter sample cell. The sample was then titrated by injecting a 1- to 2- $\mu$ l aliquot of (0.6 mM) GSNO solution at 4- to 8-min intervals. The heat evolved (kcal) per mole of GSNO added was plotted against [GSNO]/[fibrinogen]. The line represents the best fit.

determined by CD. On the other hand, both HCysNO and GSNO increased the negative ellipticity at 207 nm and decreased the positive ellipticity at  $\approx$ 190 nm, which translated to  $\approx$ 15% increase in  $\alpha$ -helix content at 50  $\mu$ M GSNO (or HCysNO). Higher RSNO concentrations could not be used owing to the absorptivity of the solutions. RSNOs also have a strong CD absorbance at 550 nm (19). When the S-NO CD signal was monitored as a function of [fibrinogen], the 550-nm absorbance decreased in a saturable manner with an estimated apparent  $K_d$  of  $\approx$ 10  $\mu$ M (data not shown).

In addition, on removal of GSNO by gel filtration chromatography, the CD spectra of fibrinogen solutions exposed to GSNO were identical to the native protein, indicating that the RSNO-induced structural perturbations were reversible.

These observations point to a mechanism where GSNO and HCysNO alter fibrinogen structure not through a chemical reaction, but instead they induce a conformational change in the protein by binding at specific site(s). We hypothesize that these RSNO-binding sites might be in regions of the protein that are disordered and rich in aromatic side chains. The requirement for GSNO-binding domains being in unstructured regions of the protein is assumed because GSNO increased the  $\alpha$ -helical

content of the protein, thus suggesting that it interacts with regions with little or no structure and induces  $\alpha$ -helix formation. The recent crystal structure (1, 2) of fibrinogen indicates that the protein consists of  $\approx$ 400-Å-long sigmoidal coiled coils that connect globular C-terminal domains with a central domain consisting of the N-terminal regions of the  $\alpha_2$ ,  $\beta_2$ , and  $\gamma_2$  subunits. Despite a large degree of structure in the protein, there are several domains that are largely unstructured. By far the most unstructured of these is the C-terminal end of the  $\alpha$ -subunits termed  $\alpha$ CA and  $\alpha$ CB. In the crystal structure of chicken fibrinogen (1),  $\alpha$ CA and  $\alpha$ CB appeared disordered in the electron density map, despite the fact that the chicken protein is shorter by 119 residues and lacks the  $10 \times 13$  repeated sequences (24, 25) that add additional floppiness to the bovine and human proteins. These  $\alpha$ C domains termed “free-swimming appendages” often interfere with crystal formation and had to be proteolyzed in the structure published by Brown *et al.* (2).

The second hypothesis is that the GSNO binding site is rich in aromatic residues. This is evidenced by the intrinsic fibrinogen fluorescence quenching by GSNO, which is attributed to energy transfer between Trp residues (excitation 290 nm; emission 330 nm) of the protein and the S-NO moiety of GSNO (acceptor-absorbance maxima 343 nm, 543 nm). We have previously observed that the fluorescence of *N*-dansylhomocysteine was quenched on its S-nitrosation (26). The quenching was attributed to energy transfer between the dansyl moiety donor (excitation 340 nm; emission 540 nm) and RS-NO (acceptor, absorbance 543 nm), and, in order for this process to occur, the RS-NO must “lay over” the dansyl ring. Recent calculations by Chen *et al.* (27) indicated that the interaction between the SNO moiety and the dansyl ring is energetically favorable.

The fact that, in the present study, the quenching of Trp fluorescence was saturable and occurred at a concentration much lower than expected for collisional quenching suggests that GSNO interacts at specific sites on fibrinogen via SNO-aromatic interactions. This binding is thought to yield conformational changes that inhibit thrombin-catalyzed fibrinogen polymerization. Examination of the protein database (PDB) files 1DEQ and 1EI3 revealed that aromatic amino acid residues are abundant in the following nonhelical structures: globular  $\alpha$ C domains, which are on or close to the central amino-terminal disulfide-knot (28), and globular C-terminal domains of B $\beta$  (twelve Trp) and  $\gamma$  (ten Trp). The  $\alpha$ C domains are likely GSNO-binding sites both from

```

Human: 20  ADSGEGDFLAXXXXXXXXXXXXXXQSACKDSDWPFCSDEDWNYKCPGRCRMKGLIDEVNO 79
          +D  GDFL                      QSACK++ WPFCSDEDWN KCPGRCRMKGLIDEV+Q
Bovine: 4  SDPPSGDFLTFEGGVRGPRLVERQQSACKETGWPFCSDEDWNTKCPGRCRMKGLIDEVDQ 63

Human: 80  DFTNRINKLNLSLFYQKNNKDSHSLTNTIMEILRGDFSSANNRDNNTYNRVSEDLRSRIE 139
          DFT+RINKL++SLF YQKN+KDS++LT NI+E++RGDF+ ANN DNT+ +++EDLRSRIE
Bovine: 64 DFTSRINKLRDSLFFNYQKNSKDSNLTNTKNIIVEIMRGDFAKANNNDNTFKQINEDLRSRIE 123

Human: 140 VLKRVKIEKVQHIQLLQKNVRAQLVDMKRLEVDIDIKIRSCRGSCSRALAREVDLKDYE 199
          +L+RKVIE+VQ I LLQKNVR QLVDMKRLEVDIDIKIRSC+GSCSRAL +VDL+DY++
Bovine: 124 ILLRRKVIEQVQRINLLQKNVRDQLVDMKRLEVDIDIKIRSCRGSCSRALAHKVDLEDYKN 183

Human: 200  QQQKLEQVIAKDLLPSRDRQHLPLIKMKPVDLVPNGFKSQKQKVPPEWKALTDMPQMRM 259
          QQQKLEQVIA ++LLPSRD Q+LP++KM + VP FKSQKQ FLEWKA +M Q
Bovine: 184 QQQKLEQVIAINLLPSRDIQYLPILKMSTITGPVPRFVKSQLQEAFLWKALLEMQQTKM 243

Human: 260  ELERPGGNEIXXXXXXXXXXXXXXXXXXPRNXXXXXXXXXXXXXXXXXXXXXXXXXXXXGA 319
          LE GG+                               PR
Bovine: 244 VLETFGGDGHARGDSVSGGTGLAPGSPRK-----PGTSSIGNVNPGSYGPSSG 292

Human: 320  TWXXXXXXXXXXXXXXXXXXXXXXXXXXXXXXXXXXXXXXXXXPRPGSTGTWNPSSSERGSAGHWTSESSV 379
          TW                               P PGS GTWNEG E GSAG W
Bovine: 293 TWNPRPEPGSAGTWNPRPEPGSAGTWNPRPEPGSAGTWNPRPEPGSAGTWNPRPE 352

Human: 380  SGSTGQWH---SESGSFRPDSFGSGNARPNNDWGTG 413
          GS G W S S STRPDS G GN R P EDWGTG
Bovine: 353 PGSAGTWNTPGSSSSFRPDSFGSGNIRPSSPDWGTG 389

```

**Fig. 5.** BLAST (nr databases) comparison of human and bovine fibrinogen  $\alpha$ -chain.

the point of lacking structure and being Trp-rich (in that there are 12 Trp between residues 291 to 610) and from being much closer to the central domain. Veklich *et al.* (28) have reported that interaction between the  $\alpha$ C fragment and  $\alpha$ C domains inhibits fibrinogen polymerization by preventing intermolecular interaction between fibrin monomers. This finding is also consistent with the 2:1 stoichiometry of GSNO–fibrinogen complexation observed here.

An examination of the homologous  $\alpha$ C domains of human and bovine fibrinogen (Fig. 5) revealed three regions (in gray) that have sparked our interest as potential GSNO-binding domains. These regions are rich in Trp and Phe as well as containing cationic Lys or Arg residues. The cationic residues in these homologous domains could be involved in additional electrostatic contacts with GSNO and HCysNO.

A BLAST search of the protein database for short, nearly exact matches to the  $\alpha$ C domains in gray (Fig. 5) has indicated the presence of these sequences in several human proteins, including A20, an endothelial Zn-finger protein induced by tumor necrosis factor (29); peripheral benzodiazepine receptor-associated protein 1; melatonin receptor 1B; short form transcription factor C-MAF; nestin; protocadherin  $\alpha$ -1; effector cell proteinase receptor 1; G-protein  $\beta$ -subunit-like protein; and general transcription factor IIIA, as well as a highly conserved phosphoenolpyruvate carboxylase (30) domain. In addition, these domains were present in several prokaryotic proteins, including DNA topoisomerase, Ala-tRNA synthase, and DNA polymerase (hepatitis B virus).

This study indicates that low molecular weight RSNOs can drastically alter fibrinogen structure without chemical reaction with the protein. Both experiments and quantum chemistry calculations (27) are in agreement that the interaction between RSNO and aromatic amino acids may contribute to the observed

GSNO–fibrinogen interactions. RSNO-dependent allosteric interactions are predicted to occur in regions of the  $\alpha$ C chains that are rich in aromatic residues, converting them to more ordered  $\alpha$ -helices. The functional consequence of these interactions is the *in vitro* inhibition of thrombin-catalyzed fibrinogen polymerization. This inhibition was also observed with serum albumin-NO. This finding suggests that the S-nitroso derivative of the Cys-34 of albumin, which is at the end of a  $\approx 9$ -Å cleft (31), is accessible to the S-NO binding peptides of fibrinogen. However, Sugio *et al.* (31), who have solved this crystal structure, suggest that the backbone conformation in solution might be different from that observed in the crystal structure, bringing the Cys-34 thiol toward the exterior of the protein (31). In support of this idea, we have recently shown that BSA-NO was able to act as a substrate for cell surface protein-disulfide isomerase (32), indicating that this residue is accessible to large proteins.

Assuming a fibrinogen:serum albumin-NO  $K_d$  of  $\approx 1$ – $3 \mu\text{M}$  (from ITC) and a reported circulating [HSA-NO] in normal adults of  $\approx 200 \text{ nM}$  (33),  $\approx 16\%$  of fibrinogen would be bound to serum albumin-NO. This result would give rise to  $\approx 10\%$  inhibition in the clotting process. The effect on fibrinogen-dependent processes at the cell surface might be larger because [albumin-NO] on the surface may be manyfold larger because many cell types contain surface receptors for serum albumin (33).

The significance of the present study is that it demonstrates that RSNOs can potentially regulate essential physiological processes via allosteric interactions, in addition to chemical interactions, with their targets.

We thank Dr. Jack Kornblatt for his assistance in the ITC studies. This work was supported by an operating grant from the Natural Sciences and Engineering Research Council (Canada) (NSERC) and the Canada Foundation for Innovation/Ontario Innovation Trust (CFI/OIT) (to B.M.).

- Yang, Z., Mochalkin, I., Veerapandian, L., Riley, M. & Doolittle, R. F. (2000) *Proc. Natl. Acad. Sci. USA* **97**, 3907–3912.
- Brown, J. H., Volkman, N., Jun, G., Henschen-Edman, A. H. & Cohen, C. (2000) *Proc. Natl. Acad. Sci. USA* **97**, 85–90.
- Wink, D. A., Cook, J. A., Kim, S. Y., Vodovotz, Y., Pacelli, R., Krishna, M. C., Russo, A., Mitchell, J. B., Jour'd'heuil, D., Miles, A. M. & Grisham, M. B. (1997) *J. Biol. Chem.* **272**, 11147–11151.
- Girard, P. & Potier, P. (1993) *FEBS Lett.* **320**, 7–8.
- Myers, P. R., Minor, R. L., Jr., Guerra, R., Jr., Bates, J. N. & Harrison, D. G. (1990) *Nature (London)* **345**, 161–163.
- Park, J. K. J. & Kostka, P. (1997) *Anal. Biochem.* **249**, 61–66.
- Konorev, E. A., Kalyanaraman, B. & Hogg, N. (2000) *Free Radical Biol. Med.* **28**, 1671–1678.
- Xian, M., Chen, X., Liu, Z., Wang, K. & Wang, P. G. (2000) *J. Biol. Chem.* **275**, 20467–20473.
- Xian, M., Wang, K., Chen, X., Hou, Y., McGill, A., Zhou, B., Zhang, Z. Y., Cheng, J. P. & Wang, P. G. (2000) *Biochem. Biophys. Res. Commun.* **268**, 310–314.
- Xian, M., Wang, Q. M., Chen, X., Wang, K. & Wang, P. G. (2000) *Bioorg. Med. Chem. Lett.* **10**, 2097–2100.
- Loscalzo, J., Smick, D., Andon, N. & Cooke, J. (1989) *J. Pharmacol. Exp. Ther.* **249**, 726–729.
- Ramirez, J., Yu, L.-B., Li, J., Braunschweiger, P. G. & Wang, P. G. (1996) *Bioorg. Med. Chem. Lett.* **6**, 2575–2580.
- Hou, Y., Wu, X. J., Xie, W. H., Braunschweiger, P. G. & Wang, P. G. (2001) *Tetrahedron Lett.* **11**, 825–829.
- Hogg, N. (1999) *Anal. Biochem.* **272**, 257–262.
- Saavedra, J. E., Billiar, T. R., Williams, D. L., Kim, Y. M., Watkins, S. C. & Keefer, L. K. (1997) *J. Med. Chem.* **40**, 1947–1954.
- Böhm, G., Muhr, R. & Jaenicke, R. (1992) *Protein Eng.* **5**, 191–195.
- Akaike, T. & Maeda, H. (1996) *Methods Enzymol.* **268**, 211–221.
- Catani, M. V., Bernassola, F., Rossi, A. & Melino, G. (1998) *Biochem. Biophys. Res. Commun.* **249**, 275–278.
- Mohney, B. K. & Walker, G. C. (1997) *J. Am. Chem. Soc.* **119**, 9311–9312.
- Mendelsohn, M. E., O'Neill, S., George, D. & Loscalzo, J. (1990) *J. Biol. Chem.* **265**, 19028–19034.
- Loscalzo, J. (1992) *Am. J. Cardiol.* **70**, 18B–22B.
- Stamler, J. S., Simon, D. I., Jaraki O., Osborne, J. A., Francis, S., Mullins, M., Singel, D. & Loscalzo, J. S. (1992) *Proc. Natl. Acad. Sci. USA* **89**, 8087–8091.
- Simon, D. I., Stamler, J. S., Jaraki O., Keaney, J. F., Osborne, J. A., Francis, S. A., Singel, D. J. & Loscalzo, J. (1993) *Arterioscler. Thromb.* **13**, 791–799.
- Doolittle, R. F., Watt, K. W., Cottrell, B. A., Strong, D. D. & Riley, M. (1979) *Nature (London)* **280**, 64–68.
- Murakawa, M., Okamura, T., Kamura, T., Shibuya, T., Harada, M. & Niho, Y. (1993) *Thromb. Haemost.* **69**, 351–360.
- Ramachandran, N., Jacob, S., Zielinski, B., Curatola, G., Mazzanti, L. & Mutus, B. (1999) *Biochim. Biophys. Acta* **1430**, 149–154.
- Chen, X., Wen, Z., Xian, M., Wang, K., Ramachandran, N., Tang, X., Schlegel, H. B., Mutus, B. & Wang, P. G. (2001) *J. Org. Chem.* **66**, 6064–6073.
- Veklich, Y. I., Gorkun, O. V., Medved, L. V., Nieuwenhuizen, W. & Weisel, J. W. (1993) *J. Biol. Chem.* **268**, 13577–13585.
- Klinkenberg, M., Van Huffel, S., Heyninck, K. & Beyaert, R. (2001) *FEBS Lett.* **498**, 93–97.
- Matsumura, H., Terada, M., Shirakata, S., Inoue, T., Yoshinaga, T., Izui, K. & Kai, Y. (1999) *FEBS Lett.* **458**, 93–99.
- Sugio, S., Kashima, A., Mochizuki, S., Noda, M. & Kobayashi, K. (1999) *Protein Eng.* **12**, 439–446.
- Ramachandran, N., Root, P., Jiang, X. M., Hogg, P. J. & Mutus, B. (2001) *Proc. Natl. Acad. Sci. USA* **98**, 9539–9544.
- Pietraforte, D., Mallozzi, C., Scorza, G. & Minetti, M. (1995) *Biochemistry* **34**, 7177–7185.